[Reprinted from BULLETIN OF THE AMERICAN METEOROLOGICAL SOCIETY, Vol. 75, No. 9, September 1994]
Printed in U. S. A.

The Experimental Cloud Lidar Pilot Study (ECLIPS) for Cloud–Radiation Research

C. M. Platt,[1] S. A. Young,[1] A. I. Carswell,[2] S. R. Pal,[2] M. P. McCormick,[3] D. M. Winker,[3] M. DelGuasta,[4] L. Stefanutti,[4] W. L. Eberhard,[5] M. Hardesty,[5] P. H. Flamant,[6] R. Valentin,[6] B. Forgan,[7] G. G. Gimmestad,[8] H. Jäger,[9] S. S. Khmelevtsov,[10] I. Kolev,[11] B. Kaprieolev,[11] Da-ren Lu,[12] K. Sassen,[13] V. S. Shamanaev,[14] O. Uchino,[15] Y. Mizuno,[15] U. Wandinger,[16] C. Weitkamp,[16] A. Ansmann,[17] and C. Wooldridge[18]

Abstract

The Experimental Cloud Lidar Pilot Study (ECLIPS) was initiated to obtain statistics on cloud-base height, extinction, optical depth, cloud brokenness, and surface fluxes. Two observational phases have taken place, in October–December 1989 and April–July 1991, with intensive 30-day periods being selected within the two time intervals. Data are being archived at NASA Langley Research Center and, once there, are readily available to the international scientific community.

This article describes the scale of the study in terms of its international involvement and in the range of data being recorded. Lidar observations of cloud height and backscatter coefficient have been taken from a number of ground-based stations spread around the globe. Solar shortwave and infrared longwave fluxes and infrared beam radiance have been measured at the surface wherever possible. The observations have been tailored to occur around the overpass times of the NOAA weather satellites. This article describes in some detail the various retrieval methods used to obtain results on cloud-base height, extinction coefficient, and infrared emittance, paying particular attention to the uncertainties involved. The above methods are then illustrated by both model simulations and by selected results from various laboratories. The ECLIPS data are shown to represent a valuable resource for cloud parameterizations in models and for model validations.

[1]CSIRO, Division of Atmospheric Research, Mordialloc, Victoria, Australia.
[2]Department of Physics and CRESS, York University, North York, Ontario, Canada.
[3]NASA Langley Research Center, Hampton, Virginia.
[4]Institute Ricerca Onde Elettromagnetiche, CNR, Florence, Italy.
[5]NOAA Environmental Technology Laboratory, Boulder, Colorado.
[6]Laboratoire de Meteorologie Dynamique du CNRS, Ecole Polytechnique, Palaiseau, France.
[7]Bureau of Meteorology, Melbourne, Victoria, Australia.
[8]GTRI–EMLEOD, Georgia Institute of Technology, Atlanta, Georgia.
[9]Fraunhofer Institute for Atmospheric Environmental Research, Garmisch–Partenkirchen, Germany.
[10]Laboratory of Physics and Climate, Institute of Experimental Meteorology, Obninsk, Kaluga Region, Russian Federation.
[11]Institute of Electronics, Bulgarian Academy of Sciences, Sofia, Bulgaria.
[12]Institute of Atmospheric Physics, Beijing, China.
[13]Department of Meteorology, University of Utah, Salt Lake City, Utah.
[14]Institute of Atmospheric Optics, Tomsk, Siberia, Russia.
[15]Meteorological Research Institute, Japan Meteorological Agency, Yatabe, Ibaraki, Japan.
[16]GKSS—Forschungszentrum Geesthacht GmbH, Geesthacht, Germany.
[17]Institut für Troposphärenforschung, Leipzig, Germany.
[18]School of Earth Sciences, Macquarie University, Sydney, Australia.
Corresponding author address: Dr. C. Martin Platt, CSIRO, PB 1, Mordialloc, Victoria 3195, Australia.
In final form 4 May 1994.

1. Introduction: The ECLIPS rationale

Although the general mean features of the global atmosphere can be simulated satisfactorily in models of the general circulation (GCMs), it is not yet possible to simulate details of the hydrological cycle and the energy budget involved to an acceptable accuracy. Some of the main problems lie in modeling, and include sufficient accuracy, the formation of clouds, their interactions with the radiation field, and the effects of precipitation.

Clouds have a major impact on the radiation budget of the planetary system, both at the earth's surface and in the atmosphere. However, it is not yet possible to simulate accurately the amount of solar and infrared energy transmitted and emitted by clouds and absorbed at the earth's surface. Without such knowledge it is obviously impossible to categorize the earth's climate accurately. Similarly, the strong radiation absorption and emission by clouds set up large heat sources and sinks in the atmosphere itself that help to drive the atmospheric system.

The representation of clouds in GCMs has thus become a major problem for scientists. At the present state of knowledge, the certainty in prediction of increased surface temperature for a CO_2 doubling is no better than a range of temperatures between about 1.8° and 5°C. Much of this uncertainty was shown by a recent comparison of models to be due to inadequate parameterization of clouds (Cess et al. 1989).

Although imperfect, recent models that have included diagnostic liquid water indicate the possibly significant changes in cloud optical properties, particularly high clouds, caused by global warming (Roeckner et al. 1987). It has been calculated that the changes in cirrus emissivity, for example, caused by a CO_2 doubling might easily be detected by a suitable ground-based or satellite monitoring program.

Similarly, simulations by Mitchell et al. (1989) indicate that a global warming will cause significant adjustments in the water/ice ratio in mixed-phase clouds. If the climate warms, some ice clouds (which precipitate quickly) will be replaced by longer-lasting water clouds. This not only will increase the cloud amount, but will change the balance between solar reflection and infrared emission.

A recognition of the major part played by the movement of both energy and water in the atmosphere has led to the formation of the Global Energy and Water Cycle Experiment, which is now the main initiative within the World Climate Research Program (WCRP). Closely associated with that program is the International Satellite Cloud Climatology Project (ISCCP). A further recent large initiative that tackles the cloud/radiation problem is the U.S. Department of Energy's Atmospheric Radiation Measurement (ARM) program. ARM plans to establish several comprehensive ground-based stations for monitoring cloud (and clear air) radiative properties and their evolution with time.

Although much has been achieved in the past two decades in the understanding of cloud properties, particularly regarding the interaction of clouds with radiation, it is clear that much remains to be done. This is because of the essential complexities of the clouds themselves and their interactions with the environment. One obvious and daily observed complexity is that clouds are often broken and, in any case, very inhomogeneous. It is found that single cumulus clouds, for instance, interact with radiation in a radically different way compared with horizontally layered clouds. Progress has been made on the properties of clouds largely through limited process studies, where the detailed radiative interactions, cloud microphysics, etc., of individual clouds, or cloud systems, have been investigated by instrumented aircraft. Much information has also been obtained on cloud microphysics by similar experiments whose aims have been to study the details of cloud formation and evolution.

Progress has also been made in the understanding of whole cloud systems and their effect on the radiation fluxes at the *top* of the atmosphere, with the powerful techniques of scanning radiometry onboard satellites. Such techniques have given extensive views of cloud systems, and much effort has been expended on interpreting satellite images.

Although much has been achieved in the past two decades in the understanding of cloud properties, particularly regarding the interaction of clouds with radiation, it is clear that much remains to be done. This is because of the essential complexities of the clouds themselves and their interactions with the environment.

The technique of lidar has provided a powerful new tool for investigating clouds, particularly when used with passive radiometers (Platt et al. 1987). The ground-based lidar and radiometer (LIRAD) method has added greatly to knowledge of the optical properties of cirrus clouds. In the recent First ISCCP Regional Experiment (FIRE) studies, lidar and scanning radiometers on board a high-flying ER-2 aircraft, as well as on the ground, provided extensive measurements of cirrus cloud properties.

However, some of the main problems involved with clouds and their radiative interactions remain. These include cloud brokenness, cloud structure, cloud-top and -base heights, and cloud extinction and optical depth. These can all be investigated to various degrees with surface-based lidar.

The above problems formed the basis for the ECLIPS project.

Originally, ECLIPS was initiated to fulfill a need: how can we obtain good datasets on cloud-base altitude? It has been recognized for a long time that satellite passive radiometer data are unable to give unambiguous information on cloud-base height. The alternative is to take observations of cloud base from the ground over a long period of time. Obviously, such cloud-base data would be to some extent characteristic of a given locality, but effects from observations in different climate regions and geographical regions should also be apparent in the data. Furthermore, in principle, observations could be made over an extended period of many years.

TABLE 1. Summary of quantities to be reported.

Required quantities
Lidar characteristics and ancillary site data
Cloud type and amount
Cloud-base height
Cloud depth or apparent depth
Lidar calibration constant
Downward infrared longwave flux
Surface pressure, temperature, relative humidity
Desirable quantities
Cloud effective extinction coefficient
Depolarization ratio
Cloud emittance
Rawinsonde data
Cloud velocity vector
Downward shortwave solar flux

ECLIPS has progressed since its original inception into a much more ambitious project. Data have also been obtained on cloud structure, extinction optical depth, and emittance. Furthermore, several novel methods have been devised to improve the quality of both cloud-base altitude and extinction data. Finally, taking into account the current interest in the surface radiation budget, the measurement of surface longwave and shortwave radiation fluxes, together with radiosonde data, would, when taken with the lidar data, form a unique set of data.

Similarly, the availability of concurrent satellite visible and infrared images would enable the validation of retrieval techniques. Thus, the study of the surface energy balance and the improvement in satellite retrievals were both built into the original aims. The landmarks and history of ECLIPS are documented in appendix A.

2. ECLIPS aims, philosophy, observational phases, and archive

The original aims of ECLIPS as formulated in the 1988 First Workshop (WMO 1988) are as follows:

- to demonstrate the feasibility of obtaining a long-term climatology of cloud base height and cloud optical properties with ground-based lidar, and to formulate a plan of long-term measurement;
- to improve methods of retrieval of cloud data from satellites by comparison of satellite and lidar data;
- to improve the prediction of the surface energy balance from satellite data; and
- to obtain a dataset of cloud optical properties that would be complementary to the ISCCP dataset.

To restrict data initially to manageable proportions and to involve as many lidar laboratories as possible, it was decided to hold two intensive observational phases of about 30 days each, separated by about 18 months and covering the two extreme seasons of late spring/summer and late autumn/winter.

It was further decided to restrict observations simply to an elastic single-wavelength lidar with accompanying surface downcoming infrared flux as minimum requirements, but with the opportunity to utilize more complex instrumentation if desired. A complete list of required and desirable variables is given in Table 1.

The dates for the two observational phases, together with a summary of observations made by each participant, are shown in Tables 2 and 3. The affiliation of each participant is given in the address list at the beginning of the article. The plan was to make at least 30 days of observations over each time period, with 3 months of flexibility in the commencement date. In some cases, laboratories had to stray outside these times because of other observational programs and commitments.

It can be seen that the response to the original invitation to laboratories to take part in ECLIPS was enthusiastic and, in some cases, additional observations to ECLIPS requirements were made. For instance, the ECLIPS observational periods were used by the team from the NOAA Wave Propagation Laboratory (now the Environmental Technology Laboratory) as a springboard to develop new cloud-sensing techniques at 10.6-μm lidar wavelength (Eberhard 1933a,b) and to develop the use of combinations of instruments with lidar, such as radar (Intrieri et al. 1993) and infrared radiometry. Eberhard et al. (1992) documented data for five observational cases as a prototype example for future ARM sites. Additional participants, particularly from eastern Europe, were welcomed in Phase II.

The importance of the data to other programs was recognized at the inception of the project, and it was agreed that data be archived in suitable formats at a central location at NASA Langley Research Center, Hampton, Virginia. A summary of the information being archived is given in appendix B, together with the address of the data archival manager from whom more detailed information can be obtained. Although the dataset from a number of laboratories is not yet complete, data presently in the archive are available to the wider community. Considerable work has gone into producing a suitable archive and to refining the format. This has occurred over several years and at

several workshops, and the format is in fact still being refined.

3. Retrieval of cloud base

a. Definition of cloud base

It soon became obvious during initial analyses of ECLIPS cloud data that the retrieval of a value for the cloud-base height was not as straightforward as was first anticipated. The reasons for this are quite complex, and it is not even certain that a single algorithm would be suitable for all cloud types at all heights. For instance, the lidar backscatter signal falls off as the square of the range, but the background sky noise remains constant. Furthermore, high clouds are much less dense than low clouds and often have superimposed a significant photon noise component. These factors reinforce to yield much lower signal-to-noise ratios for clouds in the upper troposphere. In that case, cloud-base algorithms have to distinguish between signal departures due to random noise and those due to cloud base.

Other factors can be just as problematic. Clouds often precipitate, are sometimes of mixed phase, and typically attenuate return signals from higher-level clouds. High cirrus clouds are composed of complex structures due to shear in the horizontal winds and are often convective in nature. Thus, clouds are spatially very inhomogeneous so that cloud-base altitudes can vary rapidly in one cloud system.

Further problems occur where very moist air exists below the cloud base. The growth of precondensation aerosols can cause a smooth increase of lidar backscatter before "cloud base" is even reached. All the above factors cause problems in defining cloud-base altitude, let alone measuring it.

The definition of cloud base is also influenced by various research requirements. For surface radiation budget studies, it is the radiatively important cloud base that is required. In this case, even a considerable depth of virga may not be important.

However, generally speaking, it is convenient to define cloud-base altitude as that altitude above which solid hydrometeors exist and can be detected, be they droplets, ice particles, or rain. This, of course, includes precipitating virga. Simultaneous measurements of the infrared flux at the surface can then tell observers how important the cloud virga is radiatively. Similarly, the retrieval of the cloud extinction coefficient will aid in the radiative interpretation.

It is also important to retrieve the cloud-top altitude. In the case of complete attenuation of the lidar pulse in the cloud, such as often happens in low water clouds, the retrieved cloud-top altitude is only an "effective" altitude and is defined as such in the data format. However, in cases of upper-level and some midlevel clouds, the lidar pulse can generally penetrate to cloud top. Complete penetration can often be gauged by the detection of Rayleigh scattering above cloud top, particularly for shorter-wavelength lidars, where Rayleigh scattering is enhanced.

TABLE 2. ECLIPS investigators, observational sites, and observational dates.

Principal investigator	Site	Phase I 1989	Phase II 1991
Da-ren Lu	36°56' N–116°28' E	1 Sept.–30 Sept.	
W. Eberhard	40°3' N–105° W	6 Sept.–5 Oct.	
K. Sassen	40°56' N–111°49' W	15 Sept.–30 Nov.	1 May–1 July
L. Stefanutti	66° 40' S–140° E 46°N, 02°E (Phase II)	15 Sept.–31 Oct.	10 Mar.–14 May*
P. Flamant	58°8' N–8°7' E	17 Sept.–18 Oct.	22 May–19 June
Y. Sasano	36° N–140° E	18 Sept.–20 Oct.	
O. Uchino	36° N–140° E	18 Sept.–17 Oct.	
C. Weitkamp	53°42' N–7°15' E	18 Sept.–24 Oct.	
C. Weitkamp	53°30' N–10°31' E		29 May–27 June
A. I. Carswell	43.8° N–79.5° W	18 Sept.–30 Nov.	6 June–18 July
H. Jager	47.5° N–11.0° E	9 Oct.–29 Nov.	
D. M. Winker	37.1° N–76.3° W	15 Oct.–11 Nov.	5 May–1 June
G. Gimmestad	33.78° N–84.32° W	23 Oct.–20 Nov.	
C. M. Platt	38° S–145° E	6 Nov.–12 Dec.	13 June–12 July
S. Khemelevtsov	55° N–37° E		23 May–20 June
V. Shamanaev			22 May–13 June
I. Kolev	42.65° N–23.4° E		28 May–9 July

* Daily data are available from May 1989 to December 1991 from D'Urmont Durville, located on an island several kilmeters off the coast of Antarctica (Del Guasta et al. 1993).

TABLE 3. ECLIPS Phase I and Phase II Measurements. X—Both phases. O—Phase II only. #—Phase I only.

Principle	LIDAR			Narrow field radiometer			Wide field flux			
	Bscatt	Depol Ratio	Other	Vis	IR	Microwave	SW	LW	Video	Rawinsonde
Da-ren Lu	X			X	X		X	X		X
K. Sassen	X	X			O		X	X	X	X
O. Uchino	#	#			#			#	#	#
C. Weitkamp	X		Raman							X
A.J. Carswell	X	X		X			X	X	X	X
H. Jäger	#							#		
D. M. Winker	X	X	Ceilometer				X	X	O	X
G. Gimmestad	X			X	X		X	X	X	
C. M. Platt	X	X		X	X		X	X	X	X
W. Eberbard	#	#	Radar	#	#	#	#	#	#	#
L. Stefanutti	X	X					X	X	X	X
Y. Sasano	X	X							X	
P. Flamant	X			O			X	X		
S. Kemelevtsov	X				X		X			X
V. Shamanaev	O	O		O			O		O	
I. Kolev	O									O

b. Methods developed for ECLIPS

Several methods of measuring cloud-base and cloud-top altitudes have been used successfully in the analysis of ECLIPS data, the choice of which depends generally on the magnitude of the peak cloud backscatter coefficient as compared to the Rayleigh and aerosol backscatter magnitudes at cloud base.

Four typical examples of profiles of lidar backscatter versus altitude are shown in Figs. 1a–d, in terms of the received power at the lidar receiver, and for four different cloud types. These four profiles illustrate the decrease in the received backscatter due to range (i.e., altitude) and also due to the decrease in molecular backscatter with altitude. They also illustrate the magnitudes of the various cloud backscatter signals compared to the molecular background signal and to the background noise levels, which determine to some extent the method of cloud-base retrieval used.

The backscatter profile from a low, dense stratocumulus cloud is given in Fig. 1a. This cloud has a base height of 0.9 km. The return is so strong there that the molecular and aerosol returns are negligible in comparison. Ascending in altitude, the backscatter from a midlevel cloud in Fig. 1b is still quite strong, as it is for a dense cirrostratus cloud shown in Fig. 1c. In contrast, two layers of thin, low-density cirrus clouds at altitudes of 12.5 and 14 km are shown with peak backscatter only about two to three times the molecular background (the Mount Pinatubo volcanic cloud is also shown from about 17 to 25 km).

Three methods developed for the determination of cloud base in ECLIPS are now described that exploit the typical behavior of lidar backscatter at cloud base for different types of clouds.

The first two methods work well where there is an unambiguous and appreciable increase in signal above cloud base, a property that is in fact illustrated in all the profiles of Figs. 1a–d. The first, so-called differential zero-crossing method, is illustrated in Fig. 2a. The first diagram (i) of Fig. 2a shows the full overlap of the lidar and receiver beams at z_0^1 and a deviation in signal at z_b signifying increased backscatter from a cloud. Diagram (ii) of Fig. 2a shows the first derivative, dP/dz, of the lidar backscatter power. At z_b, dP/dz changes sign from negative to positive, signifying the cloud-base altitude. A further change occurs at the cloud peak backscatter altitude z_p.

The determination of cloud top is more problematical. If the cloud is semitransparent and backscatter signals from the laser pulse above cloud top are received, then a similar technique as for the determination of z_b can be used. If complete attenuation of the laser pulse occurs in the cloud, then the backscatter

[1]The symbol z is used to define altitude. The symbol r is reserved for the more general case of range.

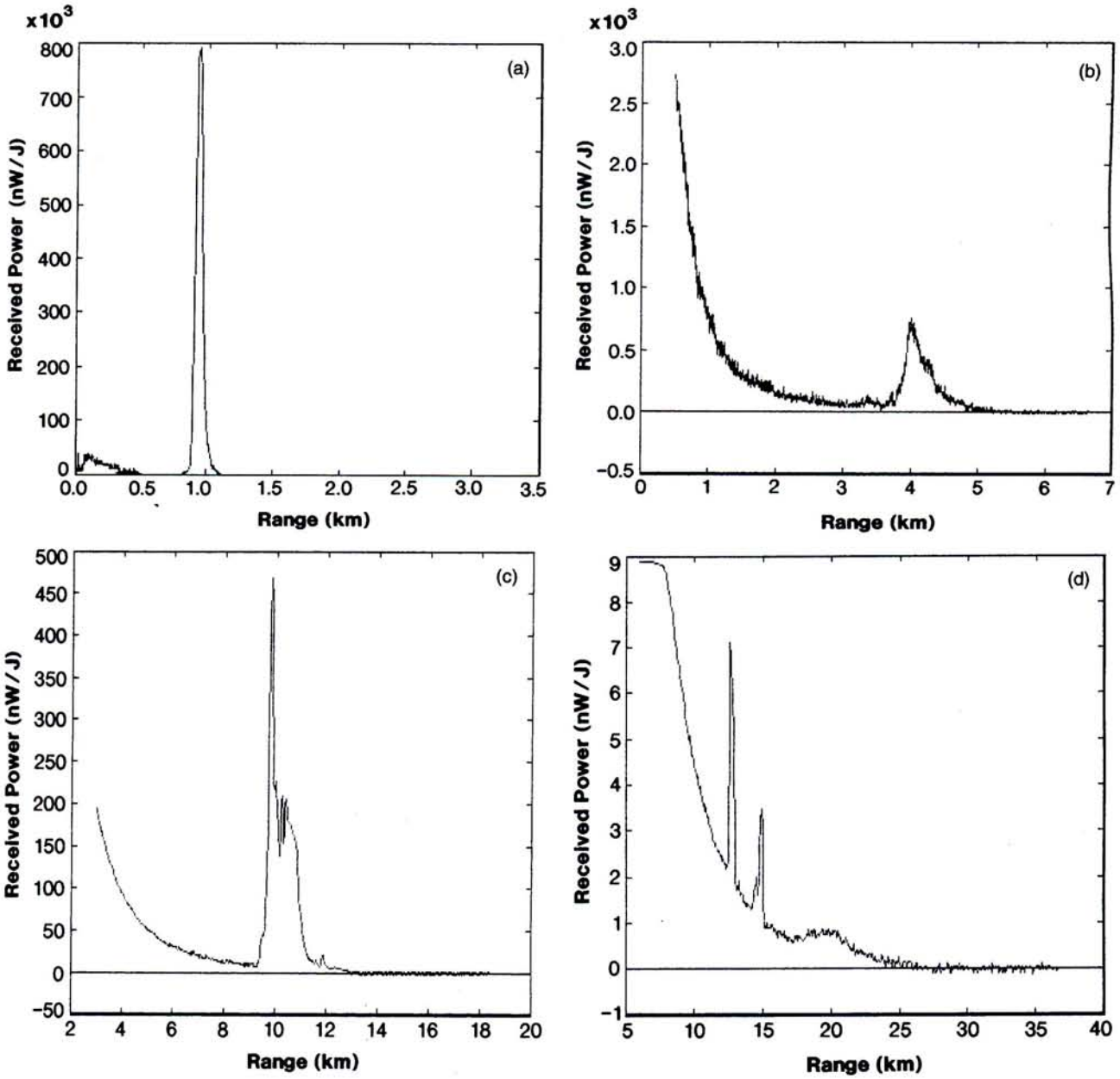

FIG. 1. Typical lidar cloud backscatter profiles uncorrected for range showing clouds at different altitudes: (a) stratocumulus, (b) altocumulus, (c) dense cirrus, (d) thin cirrus. Signal-to-noise ratios will vary somewhat with lidar power and wavelength and also, for cirrus, with the number of profiles being averaged. These profiles were obtained with a 0.532-micron laser (C. M. Platt et al. 1993).

level will decrease into the background noise. In that case, it has been agreed in ECLIPS to define an apparent height, z_t, as the height at which the signal $P(z)$ decreases below that at z_b.

The above method was reported originally by Pal et al. (1992) in which various further refinements are reported.

The second "threshold" method is illustrated schematically in Fig. 2b. The cloud-base altitude is defined as that level at which there is first an increase in signal above the clear background level and of a magnitude equal to n times the standard deviation of the background fluctuations. It is further required that the signal continues to increase, or does not decrease, for at least m successive height intervals. This latter requirement ensures that sudden noise "spikes" are not misinterpreted as cloud. The method usually calculates the standard deviation of the signal around the mean value in a small height increment Δz at altitude z, and commences to search for the cloud base by incrementing z at an altitude well below the expected cloud-base height. Values of n and m are typically 2

and 5, respectively, depending on the cloud amplitude compared to the background noise level. Of course, in the case of a cloud such as that illustrated in Fig. 1a, the fluctuations in signal below cloud base are close to zero, so that any measurable increase defines cloud base. Cloud top (or effective top) can again be determined by calculating the standard deviation of noise above cloud top, and moving downward in altitude from maximum range. Note that range-corrected values, $P(z)z^2$, can be employed instead of $P(z)$, although this will obviously increase the noise levels above cloud top.

Both methods require fine tuning by other criteria in order to avoid "triggering" of cloud base by random noise or short-term (range) spikes caused by electrical interferences or by digitization resolution. Both methods are also capable of handling multiple cloud layers and distinguishing those from layers in one cloud, that is, when $P(z)$ or $P(z)z^2$ between layers does not drop below the values at previous cloud base.

The two algorithms are obviously closely related as they both discriminate a change of slope from the decreasing (with altitude) backscatter (molecular plus aerosol) just below cloud base to the typically sharp increase in backscatter above cloud base. Both algorithms can be tuned to ignore small enhancements in backscatter below cloud "base," caused by aerosol precondensation growth, and in the case of the differential method to avoid the effects of noise fluctuations. In the case of the threshold method more sophisticated numerical filters have been developed to characterize the noise spectrum in the return signal.

The third method of cloud-base retrieval can be used for low-density clouds such as those shown in Fig. 1d. In that case, the cloud-base and -top altitudes can be retrieved more precisely by fitting the lidar profile to a calculated profile of molecular, or Rayleigh, backscatter obtained from radiosonde data. The cloud-top and -base altitudes are then retrieved automatically when the cloud backscatter increases above molecular level, although some threshold criterion will still be required.

c. Examples of derivation of cloud base and height

Figure 3 shows an example of cloud boundary retrievals in a cirrus cloud using the differential zero-crossing method. The diagram shows a time–height lidar backscatter grayscale intensity profile of a cirrus cloud for a lidar firing in the vertical. The time that a particular section of the cloud was overhead is shown on the x axis. The grayscale intensity indicates the magnitude of the lidar backscatter and its variation with altitude. The black circles indicate the retrieved cloud-base and cloud-top heights. Figure 4 shows the cloud-base and cloud-top heights retrieved using two collocated lidars of different wavelength, one at 0.694 μm (ruby) and one at 10.6 μm (CO_2). The agreement is quite good, but there are some periods, at cloud top, where differences occur. This phenomenon may be due to the presence of rather small particles near cloud top particularly from about 2005 to 2035. The smaller particles, if less than 10 μm in size, would give a smaller backscatter at 10.6 microns which could give an apparently lower cloud top.

Figure 5 shows the cloud-base distribution with altitude measured by Kolev et al. (1993) in their ECLIPS (Phase II) experiment, given as the numbers of occurrences between various height ranges. Two cloud groups are noted, one at 700 to 1200 m and another at 2000 to 2600 m. These two groups are related to the thermodynamics of the atmospheric boundary layer and to the formation of fair-weather cumulus at the higher altitudes. There may have been cases when clouds in the lower height group were obscuring

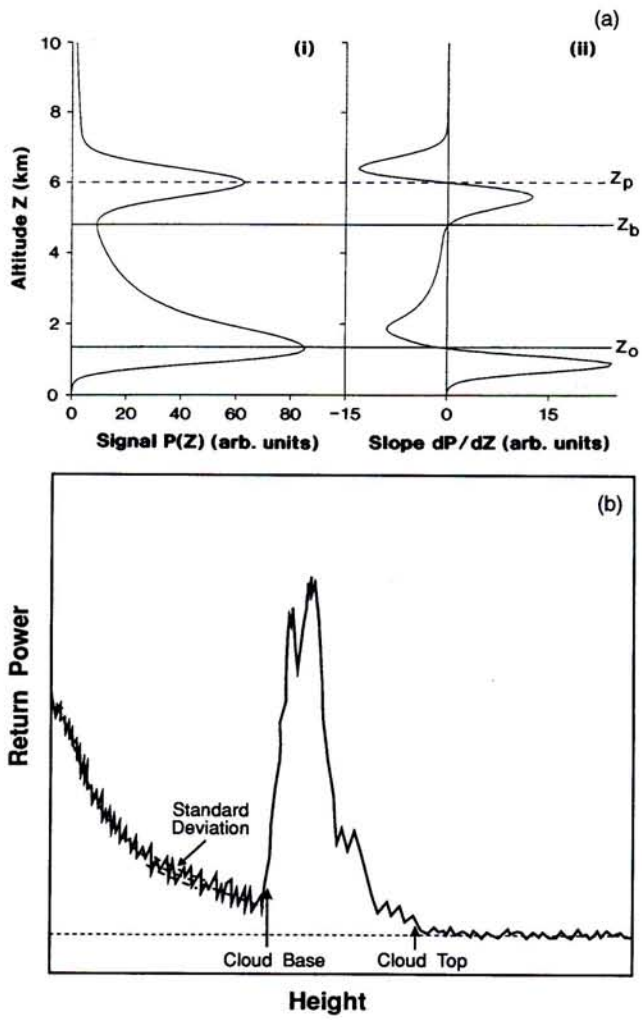

FIG. 2. Schematic representation of techniques for automatic retrieval of cloud-base and -top heights: (a) the differential zero-crossing method (after Pal et al. 1992); (b) the threshold method.

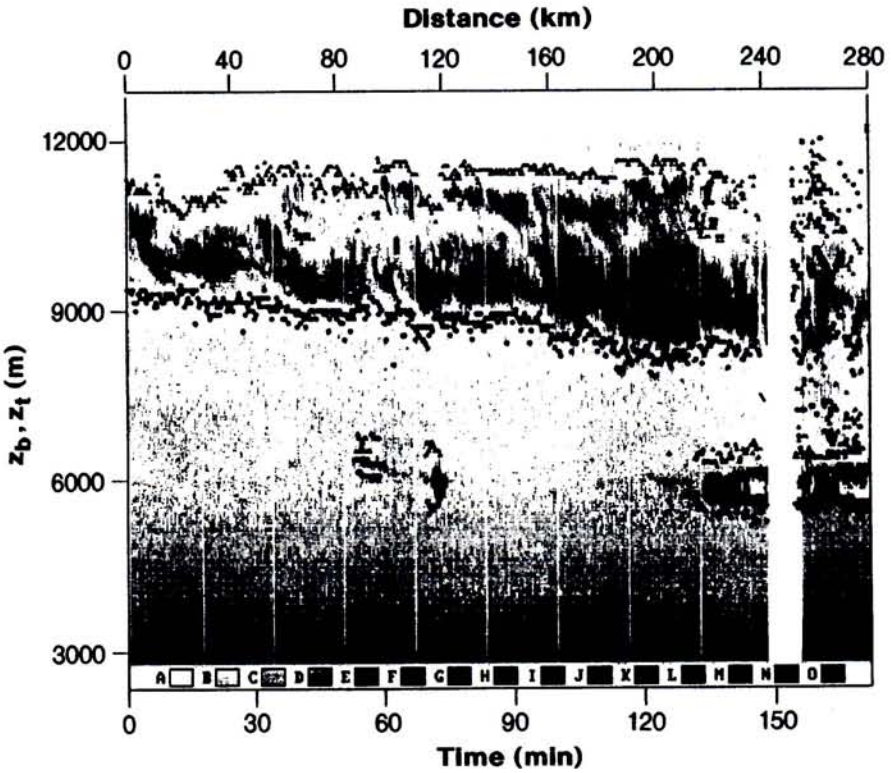

FIG. 3. Time–height grayscale intensity representation of lidar profiles of cirrus and midlevel clouds, together with retrieved bases (dots) and heights (triangles) using the differential zero-crossing method (Pal et al. 1992).

the higher clouds, so that the frequencies observed in this top group should be treated with caution.

Sassen and Cho (1992) reported using the third cloud-base retrieval method for thin cirrus retrievals, fitting their data to the Rayleigh backscatter profile calculated from radiosonde data, on the assumption of negligible aerosol backscatter at some chosen altitude. An example of a retrieval of thin cirrus cloud from that paper is shown in Fig. 6. The backscatter coefficient has been calculated from the scattering ratio. The cloud-top and -base heights are shown clearly. This method of Sassen and Cho's was also used by them to retrieve the cloud extinction coefficient, as described in section 4e. The method thus retrieves several ECLIPS variables simultaneously, and it can be used for any cirrus case where the optical depth is small and there are measurable Rayleigh backscatter returns from above cloud top.

More complicated situations in which snow is falling from a supercooled cloud layer in a mountain storm have been investigated by Sassen and Zhao (1993). The differential zero-crossing method is used in conjunction with a minimum depolarization ratio, which distinguishes snow from the supercooled base.

In summary, it should be emphasized that no method is entirely watertight. Cases of low cloud will occur where the cloud backscatter is quite weak, and when the method for low-density cirrus clouds might be more appropriate, and vice versa.

As found by Sassen and Zhao, the linear depolarization ratio (Δ) is another quantity that holds out promise when used in combination with "standard" methods. The value of Δ for Rayleigh scattering is negligible, a fact that can sometimes assist in the recovery of cloud boundaries. Cirrus clouds have values of Δ in the range of from 0.3 to 0.5 throughout the cloud in most cases; thus, the cloud base can be determined unambiguously in those cases. In water clouds, Δ is very low (~0.016) at cloud base, but rises above cloud base due to multiple scattering, so that again the cloud-base altitude is defined. Application of this method must await a greater understanding of the ranges of Δ values in various clouds.

d. Measurement of cloud base at other wavelengths

Even taking into account the physical problems involved in defining cloud base, which have been discussed previously, the use of other sounding wavelengths may cause a non-uniqueness in the definition of cloud base or cloud top. For instance, at visible

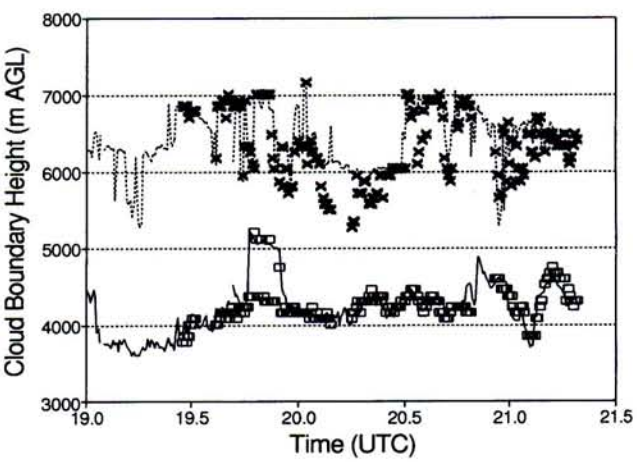

FIG. 4. Retrieved cloud bases and tops for a deep midlevel cloud using the threshold method with two lidars at different wavelengths. Lines are from a ruby lidar at 0.694 micron and squares and crosses from a CO_2 lidar at 10.6 μm. (Eberhard et al. 1992).

wavelengths, the cloud particles are always larger than those wavelengths, and so the scattering efficiency is a maximum and proportional to the cloud particle cross section. For infrared wavelengths, say at 10 μm, the wavelengths are now larger than the small cloud particles less than 10 μm, and so the scattering cross sections can decrease. Thus, infrared lidars could "miss" layers of very small particles (e.g., see Fig. 4). For radar wavelengths, say for a millimeter radar with a wavelength of 8 mm, the scattering efficiencies are much lower, although millimeter radars are very sensitive coherent devices. Cloud droplets near cloud base in a nonraining cumulus-type cloud tend to be small, as the particles grow as they rise, and therefore it is possible that a millimeter radar may measure a higher cloud base than lidar. In cirrus ice clouds where the ice particles tend to be descending, the large particles tend to be near cloud base and easily detectable by millimeter radar, although very close to cloud base particles would be evaporating.

In conclusion, a visible lidar will give a clear and unambiguous signal for small cloud particles, and therefore, taking into account the various problems with actually *defining* cloud base will give the best measurement. The use of infrared lidar or millimeter radar could cause some ambiguity, although millimeter radar has the virtue of superior cloud penetration.

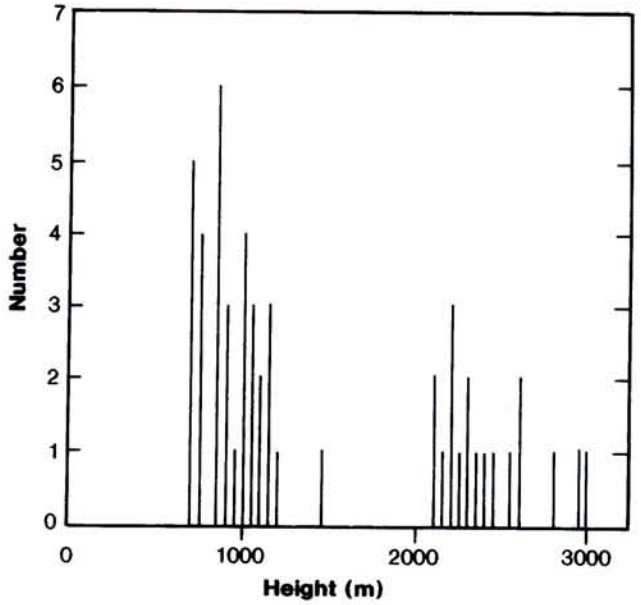

FIG. 5. Frequency histograms of the number of cases of retrieved cloud base at different altitudes for stratocumulus and cumulus clouds (Kolev et al. 1993).

4. Retrieval of extinction coefficient

a. General comments

One of the primary motivations for the ECLIPS program was the need to improve our understanding of the role of clouds in the transfer of radiation through the atmosphere. The optical extinction of clouds is a key parameter in radiative transfer and therefore considerable effort has recently been put into its retrieval. The ECLIPS program has continued this work and has made some further progress.

Lidar has the potential for making remote measurements of the atmospheric extinction with excellent spatial and temporal resolution. However, accurate inversion of the lidar equation imposes fairly stringent requirements on calibration and on boundary values, and, in the case of retrieval of backscatter coefficient, on knowledge of the extinction-to-backscatter ratio. Further assumptions have to be built into the retrievals, such as a constant value of the extinction-to-backscatter ratio, together with theoretically computed values of multiple scattering effects. However, as will be demonstrated in what follows, single-channel lidar retrievals can still give meaningful results, particularly for clouds with optical depths of less than about 3, and also for limited ranges of altitude above cloud base for clouds of high optical depth.

b. Methods adopted

At the third ECLIPS workshop (see appendix A), it was accordingly agreed that simple inversion meth-

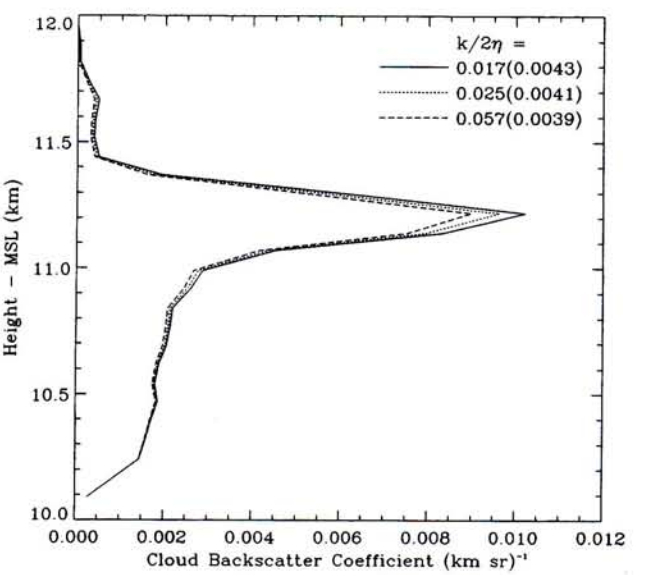

FIG. 6. A retrieved cloud profile of backscatter coefficient for a very thin subvisual cirrus. The cloud-base and cloud-top altitude are measured where the signal decreases to zero. The Rayleigh scattering has been eliminated. Here $k/2h$ is the isotropic backscatter-to-extinction ratio divided by twice the multiple scattering factor (Sassen and Cho 1992).

ods should be used to retrieve the cloud volume extinction coefficient where single-channel lidars were operated. For other cases, where there were independent datasets, more complex methods could be used (e.g., see section 4f). Most of the methods that have been developed are related to each other, depending as they do on the solution of the standard lidar equation and upon the fact that there are generally two unknowns, the backscatter and extinction coefficients that have to be related in some manner, either empirically or theoretically, in order to invert the lidar equation. There have been many discussions regarding the solutions of the lidar equation and details will not be discussed here (e.g., Barrett and Ben-Dov 1967; Viezee et al. 1969; Davis 1969; Fernald et al. 1972; Platt 1973, 1979; Klett 1981; Fernald 1984). It was evident quite early on that molecular scatter could often be ignored compared to the dominant cloud-particle scatter, and a so-called single-component atmosphere was often used to describe scattering within a cloud and to retrieve the cloud backscatter and extinction coefficients (e.g., Davis 1969; Platt 1973, 1979). However, in the case of mildly turbid atmospheres such as aerosols or thin cirrus, molecular scatter must also be included. The resultant two-component solution was obtained first by Fernald et al. (1972).

Solutions to the lidar equation exist that use either the variables $X(z) = P(z)z^2$ or $S(z) = \ln[P(z)z^2]$, referred to as linear and logarithmic solutions, respectively (e.g., Platt 1979; Klett 1981; Fernald 1984). The linear solution has advantages where noisy data produce negative values of $P(z)z^2$.

Solutions can be found for either the extinction coefficient σ or the backscatter coefficient β. In the former case, the solution is most accurate for dense clouds such as cumulus, and the backscatter-to-extinction ratio k, equal to β/σ, is eliminated from the solution, provided that k is constant throughout the cloud. In the latter case, the solution is more accurate for clouds of low optical depth such as cirrus, but a value of k is required with an accuracy that depends on the optical depth; k is also required, of course, to convert β to extinction coefficient σ.

Both the accuracy and stability of lidar retrieval solutions are naturally important and these aspects have been considered by a number of authors (e.g., Platt 1979; Klett 1981; Fernald 1984; Carnuth and Reiter 1986; Bissonnette 1986; Qiu 1988; among others). Forward solutions of backscatter coefficient β were found to become rapidly unstable for optical depths greater than about unity unless the backscatter-to-extinction ratio was specified with extreme accuracy (Platt 1979). Klett (1981), in a landmark paper, showed that a *backward* solution of either β or σ and starting above cloud top was inherently stable. However, Fernald (1984) showed that stability does not necessarily mean accuracy. The boundary values of either σ or β at cloud top still need to be specified with an accuracy that depends on the optical depth. Only when the cloud becomes very turbid does the backward solution become accurate, even when the boundary value of σ is not accurately known at least for some distance below cloud top. In that case, extinction can be obtained with an uncalibrated lidar. At the other extreme, either forward or backward solutions are reasonably accurate in mildly turbid atmospheres, but an accurately calibrated lidar, together with fairly exact boundary conditions, is still required.

The effects of inaccurate specification of boundary values on the retrieved values of extinction coefficient σ have been studied by Qiu (1988) over a wide range of conditions and for both forward and backward retrievals. His numerical results, taken from his graphs, are shown in Table 4. Qiu specified σ_0 and σ_m as the boundary value extinction coefficients for the forward (σ_0 specified near cloud base) and backward (σ_m specified near cloud top) solutions, respectively. The ratio X_0 is defined as σ_0/σ_0^* where σ_0 and σ_0^* are the specified and exact values, respectively. Similarly, X_m is defined in terms of equivalent values of σ_m and σ_m^*. Incorrect specification of either σ_0 or σ_m (X_0 or X_m different from unity) leads to errors in the retrieved cloud optical depth τ_c, where τ_c is the integral of σ from cloud base to cloud top. The ratios R_0 and R_m are here both defined as τ_c/τ_c^*, where τ_c and τ_c^* are the retrieved and exact values of the optical depth, respectively.

Table 4 is then read as follows: if the cloud optical depth τ_c^* is 3.0, and $X_0 = 0.85$ (σ_0 is too low by 15%) then for the forward solution, $R_0 = 0.3$. In that case, the retrieved value, τ_c, is only 30% of the exact value. This result can be contrasted with the backward solution, where for $\tau_c^* = 3.0$ and $X_m = 0.8$, $R_m = 0.98$, and the solution has good accuracy. Of course, in this case, there has to be sufficient molecular backscatter signal from above cloud top to specify σ_0 to 20% accuracy.

Regions where the forward solution becomes unstable are left blank. The backward solution is seen to be always stable, and the accuracies are generally quite good when τ_c^* is greater than unity. At the lower values of optical depth, the backward solutions can still be reasonably accurate if there is sufficient Rayleigh molecular backscatter above the cloud (together with radiosonde data) to allow specification of a value of X_m that is reasonably close to unity. In the case of the forward solution, specification of β_0 requires an accurate calibration of the lidar, which again depends on a region of low aerosol and strong Rayleigh backscatter signals, but this will also give reasonably accurate results.

TABLE 4. Errors in lidar retrievals (after Qui 1988). See text for explanation.

Forward solution R_0							Backward solution R_m						
X_0	t_c^*	0.1	0.5	1.0	2.0	3.0	X_m	t_c^*	6	3	2	1	0.5
0.85		0.82	0.75	0.59	0.44	0.30	0.5		0.95	0.85	0.80	0.70	0.58
0.90		0.85	0.82	0.67	0.51	0.39	0.6		0.97	0.92	0.87	0.75	0.68
0.95		0.98	0.86	0.82	0.65	0.47	0.7		0.99	0.96	0.91	0.80	0.77
1.00		1.00	1.00	1.00	1.00	1.00	0.8		1.00	0.98	0.94	0.90	0.85
1.06		1.05	1.06	1.18	>4	>4	0.9		1.00	0.99	0.96	0.92	0.91
1.10		1.10	1.14	1.47			1.0		1.00	1.00	1.00	1.00	1.00
1.15		1.15	1.25	2.4			2.0		1.06	1.11	1.11	1.29	1.46
1.20		1.20	1.38	>4			3.0		1.10	1.18	1.18	1.49	1.80
							4.0		1.12	1.23	1.23	1.63	2.00

The retrieval of extinction coefficient must also take account of multiple scattering of radiation in the lidar beam (e.g., Platt 1981). This has the effect of reducing the retrieved extinction coefficient σ to a value $\eta\sigma$, where the multiple scattering factor η is less than unity. Multiple scattering thus allows greater pulse penetration into highly attenuating clouds, but it also has to be estimated in order to retrieve a value of σ; η can be estimated at present to within about 15% for low stratocumulus clouds and 25% for high cirrus clouds, but there is no fundamental obstacle to more accurate estimates in the future. Values of η range typically from 0.7 for stratocumulus to 0.4 for cirrus.

c. Stratocumulus clouds

We now consider the actual retrieval of cloud extinction coefficient for three different cloud types—stratocumulus, midlevel, and high cirrus clouds. Retrieval of extinction in stratocumulus was first considered by Lindberg et al. (1984) and Carnuth and Reiter (1986). They both utilized the fact that the Klett backward integration converges to accurate values of σ for some distance above cloud base for quite a wide range of values of σ_m (e.g., see Table 4). Lindberg et al. demonstrated that lidar values of σ give qualitative agreement with in situ measurements, at least for very turbid clouds. Kolev et al. (1989) also examined stratocumulus backscatter coefficients. A simulation of a Klett retrieval, using a model stratocumulus, is illustrated in Fig. 7a. The solution converges very well to some 100 m above cloud base, but above that, the solution becomes widely divergent. Stratocumulus is typically from 100 to 500 m deep, so that more often than not, the total optical depth of the cloud cannot be obtained. However, the rate of growth of σ immediately above cloud base can be related to various physical growth mechanisms that can themselves be related to the concentration of cloud condensation nuclei. The height in the cloud backscatter profile at which σ_m is specified is not critical, the only requirement being a sufficient signal-to-noise ratio. The effects of multiple scattering are shown in Fig. 7b. Platt (1981) found that the multiple scattering factor η in stratocumulus increased from a value of about 0.5 near cloud base and leveled off with a value of about 0.7 when the optical depth became greater than unity.

d. Midlevel clouds

The optical depths in midlevel clouds, which are often of mixed phase, have hardly been studied, and furthermore, one must distinguish between deep frontal clouds and thin altocumulus. In the latter case, and assuming a typical optical depth value of about 1. (e.g., Platt and Bartusek 1974), it can be seen from Table 4 that an accuracy in τ_c to within about a factor of 2 is possible, provided than X_m is within a factor of 2 to 3 in the backward integration. It is hoped that sufficient data are obtained from ECLIPS observations to assess the optical depths of midlevel clouds in more detail (e.g., Platt et al. 1993).

e. Cirrus clouds

High cirrus clouds often possess optical depths of less than 1 (Platt et al. 1987) and are thus semitransparent to a lidar pulse (e.g., Figs. 1c and 1d). Two-component retrieval techniques (cloud and Rayleigh

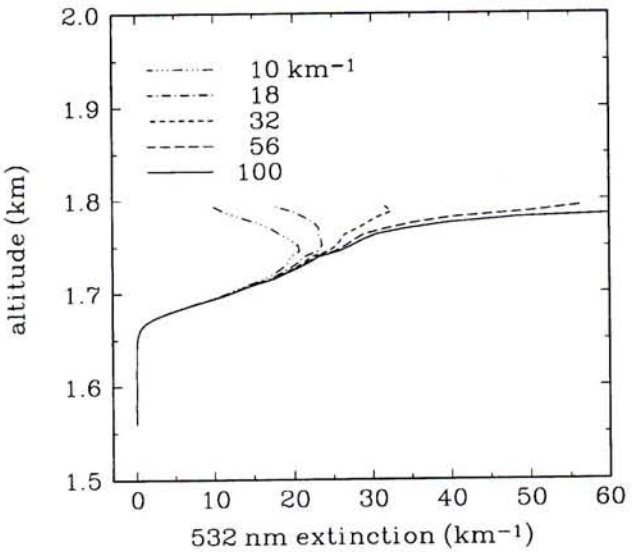

FIG. 7a. Retrieval of the cloud extinction coefficient for a dense stratocumulus cloud and for different boundary values (s_m). The solution is seen to converge for some distance above cloud base (D. Winker, private communication).

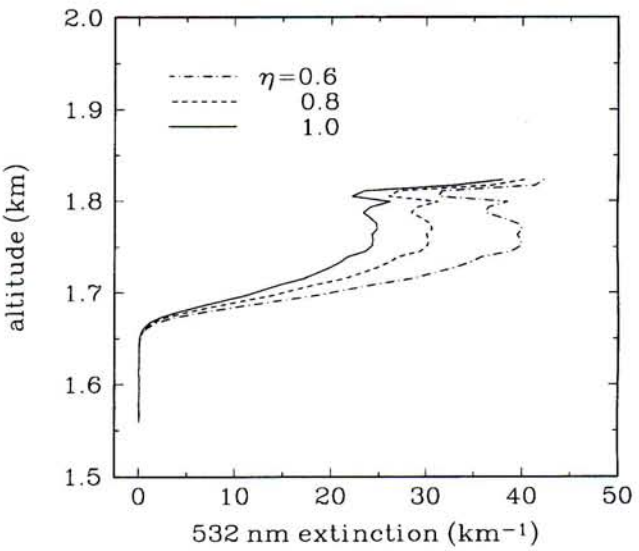

FIG. 7b. The effect on the retrieval of the extinction coefficient s of including a multiple scattering factor h for three values of h (D. Winker, private communication).

scattering) can then be utilized that employ the lidar backscatter returns from both below and above the cloud to specify either σ_0 or σ_m in forward or backward integrations, respectively. The returns can be quantified in terms of Rayleigh scattering calculated from radiosonde data with some assumptions made about aerosol backscatter (e.g., Gras et al. 1991). The errors involved in the retrieval of extinction coefficient in a cloud of very low optical depth ($\tau_c = 0.11$) are illustrated in the work of Sassen and Cho (1992) (Fig. 6). These authors used a retrieval containing both cloud and molecular scatter, after the method of Fernald (1984), to retrieve the cloud backscatter coefficient. For this method, as explained in section 4b, the cloud particle backscatter-to-extinction ratio needs to be determined or known a priori. For such low optical depth clouds, it can be seen that a variation of a factor of 3 in the backscatter-to-extinction ratio $k/2\eta$ (which includes the multiple scattering factor η) gives little change in β. A more serious factor can be the specification of the boundary value backscatter coefficien β_m. A fractional loading of aerosols in the assumed molecular atmosphere is found to cause an equivalent fractional error in β.

As mentioned previously, the multiple scattering factor η can be less than 0.5, particularly in thin cirrus (Platt 1981), leading to further uncertainties in σ (but not β). Again, this is an area that requires considerably more research.

A comprehensive set of data representing retrieved values of extinction coefficient in Antarctic clouds is illustrated in Fig. 8 (Del Guasta et al. 1993). The range of temperatures is seen to be considerable, with some dependence of σ on temperature similar to that obtained by Platt and Harshvardhan (1988) (see below). Del Guasta et al. used a standard two-component method (e.g., Fernald 1984) using Rayleigh backscatter from both above cloud top and below cloud base for their values of σ_0 and σ_m. They estimated errors in retrieved values of optical depth of up to a factor of 2, although clouds with optical depths greater than 3 were not considered. Their spread in results at any temperature was generally much greater than their stated error, thus indicating variability in cloud optical properties at any one temperature considerably greater than the estimated accuracy. This aspect agrees with the previous results of Platt et al. (1987). Once again, the effects of multiple scattering need to be considered. However, these effects will depend on the pattern of Rayleigh backscatter above the cloud, as well as particle scatter within the cloud, and this aspect has yet to be studied.

As the values of extinction coefficient in Fig. 8 vary by over four orders of magnitude, the 100% stated error is small by comparison. Thus, Fig. 8 provides a very valuable set of meaningful data.

f. Use of independent datasets

The search for more accurate retrieval methods has led to the use of supplementary, independent information, either in the form of separate lidar channels or a separate spectral radiometer. Two such methods that were used in ECLIPS are described below.

In the first method, Ansmann et al. (1992) employed a second reception channel on their lidar and measured the Raman-shifted signal from atmospheric nitrogen. The primary signal was at 308-nm wavelength in the ultraviolet and their Raman backscattered signal from nitrogen at 332 nm. In this manner they were able to discriminate between the cloud backscatter and extinction coefficients, and thus determine the profile of the cloud extinction-to-backscatter ratio. They found that this ratio is by no means constant, a finding previously suspected by Platt et al. (1987). An example of the retrieved extinction-to-backscatter ratio through a cirrus cloud is shown in Fig. 9. The ratio is seen to vary quite markedly through the cloud depth. Obviously, variations in the ratio will affect the retrieval of extinction coefficient by more than a trivial amount. The retrieval required an integration of Raman lidar returns through 9 minutes with a vertical resolution of 300 m. The Raman method could be used only at night. For daytime observations, a Klett retrieval method was employed.

The Raman technique of Ansmann et al. (1992) obviously represents a significant advance in the retrieval of cloud properties, particularly optical depth. Their nighttime data should represent valuable information for other ECLIPS users as to the accuracy and representatives of the various approximations used in the retrievals.

In the second method, Platt et al. (1987) employed a narrow beam spectral infrared radiometer measuring cloud radiance continuously in a 1-μm spectral band at a selected mean wavelength of 10.84 μm in the 8–13-μm atmospheric window. By combining lidar and radiometer observations in the so-called LIRAD method, they were able to retrieve the cloud emittances and optical depths of both cirrus and midlevel clouds, with maximum errors of 20% to 30% for small cloud emittances, decreasing to 10% for emittances approaching unity. Platt et al. were also able to retrieve effective cloud backscatter-to-extinction ratios (including multiple scattering) by using a calibrated backscatter lidar and plotting integrated attenuated backscatter versus infrared emittance. The integrated backscatter tends to the value of the isotropic backscatter-to-extinction ratio as the emittance tends to unity. Using a forward Fernald-type integration, the backscatter and extinction coefficients at the lidar wavelength were also retrieved to an estimated accuracy of about a factor of 2, an estimate that includes correction for multiple scattering. It should be pointed out that the LIRAD method is suitable for many midlevel, and most cirrus, clouds for optical depths up to 1 or 2 in value.

Although two- and multichannel techniques hold promise of more accurate retrieval of cloud extinction, the allowance for multiple scattering effects still remains as a challenge in all the techniques considered, and that is where future progress is particularly needed.

g. Ranges of application

The importance of the single-channel inversion technique, recommended for the ECLIPS (section 4a) for the retrieval of cloud extinction coefficient and optical depth, is encapsulated in the results of Del Guasta et al. (1993), illustrated in Fig. 8. Within the stated maximum error of a factor of 2, and for an optical depth of less than 3, the authors have been able to capture the main features—that is, the great variability of the extinction coefficient, as well as its trend with temperature.

The ranges of applicability of single-channel inversions have been shown in Table 4. For a typical high-power lidar system operating in the visible spectrum at about 0.5 micron, it is possible to measure sufficient Rayleigh scattering above cloud top to invert the lidar equation for cloud optical depths up to 2 or 3 in value.

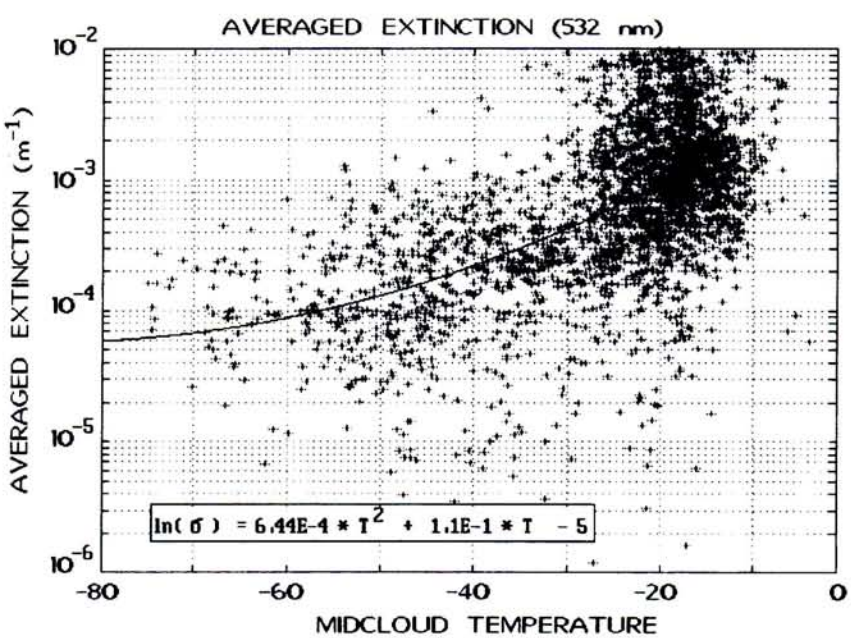

FIG. 8. Retrieved values of the extinction coefficient against midcloud temperature for Polar clouds. (Del Guasta et al. 1993). Cloud optical depths are restricted to values less than 3.0. The expression in the box shows a fit of the averaged extinction *s* against temperature.

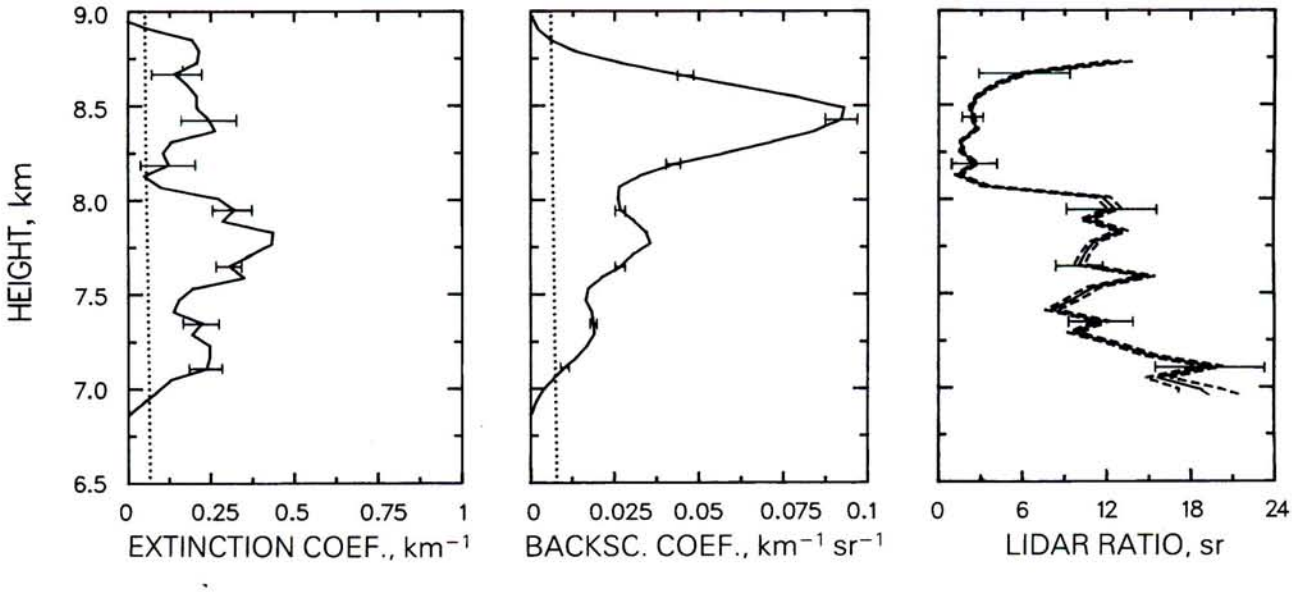

FIG. 9. Variation of cloud extinction and backscatter coefficients and extinction-to-backscatter ratio (lidar ratio) through a cirrus cloud using Raman lidar, illustrating the variation in the ratio that can occur (Ansmann et al. 1992). The dotted lines in the first two panels indicate Rayleigh extinction and backscattering profiles. Errors introduced by the uncertainty of ozone absorption of the lidar pulses are shown as dashed lines in the right-hand panel. The error bars give the estimated errors in retrieval.

For example, even for a Rayleigh signal, which can only be estimated to within a factor of 2 (X_m = 0.5 to 2.0), Table 4 indicates that a cloud optical depth of 3.0 can be retrieved to within 15% of its true value. At lower optical depths, a better estimate of the Rayleigh signal is possible and comparable accuracy is obtainable.

In dense clouds with optical depths greater than 10, the increase in extinction coefficient can be obtained quite accurately until complete pulse attenuation occurs as illustrated in Fig. 7a.

Use of independent datasets, as discussed in section 4f, will yield accurate data on cloud infrared emittances, infrared optical depths, and backscatter-to-extinction ratios.

Uncertainties in multiple scattering factors will cause further errors of some 15% to 25% as discussed in section 4b. However, this is a region where there are no fundamental obstacles to future progress in reducing errors from this cause.

5. Fluxes and radiances at the ground: Cloud emittance

The absorption of longwave and shortwave radiation at the earth's surface is a vital quantity in the determination of regional and global climate. The downward radiation, and particularly the net radiation at the surface, are influenced considerably by the presence of clouds. In the case of solar shortwave radiation, the modulation by clouds is determined largely by the cloud optical depth, whereas the infrared flux is determined mainly by the cloud-base altitude. For this reason, the longwave flux is considered to be a required observation (Table 1), whereas the solar flux was categorized as a desirable observation. However, lidar observations made during ECLIPS without any surface fluxes were still considered to be very useful. A major problem in the computation of fluxes at the surface is the estimation of flux from broken cloud fields. With the availability of all-sky imaging (described in section 8) together with lidar and radiometer data, the observed longwave and shortwave fluxes provide a valuable dataset for the validation of models.

The Baseline Surface Radiation Network (BSRN) program aims to improve the prediction of the surface radiative fluxes. ECLIPS aims to support this program by supplying appropriate validation data, and the BSRN community has shown considerable interest (WMO 1992).

The measurement of the infrared longwave flux is subject to errors and uncertainties during the daytime when solar radiation has to be either blocked or measured separately and subtracted. The uncertainties in the longwave measurements are then a maximum of about 10 W m^{-2} (Brogniez et al. 1986). Associated with the measurement of longwave fluxes is the desirability of radiosonde data taken at, or near to, the observation site.

Additional to the longwave flux, the downward-beam radiance in the thermal window (in a suitable

spectral filter pass) was recommended as a desirable quantity for several reasons. The chief reason, as described in section 4f, is that for a semitransparent cloud, it enables the calculation of the cloud infrared optical depth δ_λ in a narrow wavelength interval $\Delta\lambda$. This calculation is more accurate than the inference of the visible optical depth from lidar measurements alone because of the inherent difficulties already discussed of retrieving accurate extinction coefficients and optical depths from lidar backscatter data. Another reason is that the beam radiance can be correlated directly with the total longwave flux from the cloud. Because the cloud absorption coefficient, and therefore emittance and scattering albedo, is spectrally dependent in the atmospheric window and is also dependent on cloud particle phase (water or ice), a comprehensive measurement of cloud infrared optical depth would require measurements with an infrared spectrometer. However, the emittance in one spectral band (say 10–12 μm) can be related to the other window wavelengths by theoretical models. Furthermore, theory shows that the 10–12-μm radiance is equivalent to the total cloud greybody emittance (Platt and Stephens 1980).

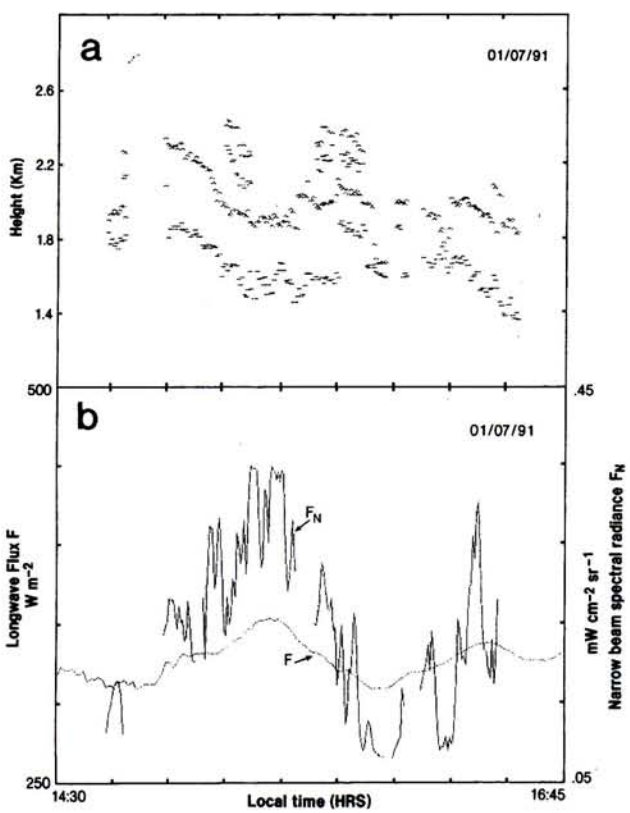

FIG. 10. Infrared fluxes measured at the surface below a midlevel cloud. (a.) Cloud boundaries retrieved with the threshold method showing cloud base and top and some multiple layering. (b.) Longwave infrared flux and narrowband window infrared radiance (10–12 μm), showing that the cloud is nonblack with an emittance generally less than unity (Platt et al. 1993).

Figure 10 shows a composite diagram of the cloud-base and -top altitudes of a typical cloud and associated longwave flux and beam radiance. In Figure 10a, the cloud-base and cloud-top altitudes are shown for every minute. The time covers the period during which intensive observations were taken for one hour on each side of a satellite overpass. Figure 10b shows the corresponding broadband infrared flux and the narrow beam filter (10.84 μm) vertical radiance plotted on the same axis. Although the flux is smoothed out to some extent, as expected, there is still a correlation with the vertical radiance at 10–12 μm. This can be expected because cloud broadband fluxes reaching the ground will be mainly in the 8–12-μm atmospheric window, and furthermore, radiation emitted near to the vertical direction will suffer the least attenuation. The variable emittance of the cloud, reflected in the variable radiance, is evident. Figure 11 shows another example of longwave and shortwave fluxes and cloud backscatter in a field of boundary layer cloud. In the latter, substantial changes in shortwave radiation are seen to occur, due to considerable variations in cloud optical depth. Changes in infrared flux, however, are much less.

6. Depolarization ratio

The lidar depolarization ratio is a measure of the depolarization of the linearly polarized lidar pulse. It is caused either by internal reflections in ice crystals or other irregular particles or else indirectly through multiple scatter radiation in water clouds. It is listed in Table 1 as a desirable quantity, and many lidars have the capability to make this measurement.

In highly attenuating water clouds, the depolarization ratio increases monotonically from a very low value at cloud base (a few percent) to quite high values (~0.3 to 0.5) within 100 m of cloud base. A recent paper by Sassen et al. (1992) demonstrates this behavior. In high cirrus ice clouds, the depolarization ratio increases immediately above cloud base to values between about 0.2 and 0.6, and tends to vary more with particle shape and habit than optical depth (Platt et al. 1987). In the case of midlevel clouds, both ice and water phases are present and lidar can discriminate between the two phases (but again making allowances for multiple scattering). The depolarization ratio can obviously increase the information content of lidar considerably (e.g., see section 3), and is therefore a very useful and thus desirable quantity in ECLIPS.

7. Satellite data

One of the goals of ECLIPS was to provide ground truth or, more correctly, air truth data for comparison with simultaneous satellite retrievals. Previous comparisons between satellite data and ground-based lidar and radiometer data have shown that the satellite data can be navigated well enough to compare with vertical lidar data (e.g., Platt et al. 1980). More recently, Minnis et al. (1990) have used combined satellite and lidar data in the FIRE experiment to derive cirrus optical properties. Similar comparisons were made by Stone et al. (1990).

The minimum requirement for the ECLIPS intensive periods was to take observations for a period of a few hours, centered on a National Oceanic and Atmospheric Administration (NOAA) satellite overpass. The NOAA satellites carry the Advanced Very High Resolution Radiometer (AVHRR), which has five filter channels in the visible and the infrared, two of which occur in the infrared atmospheric window. Thus the satellite-derived cloud optical properties can be compared with those derived from lidar, LIRAD, or from the measured longwave or shortwave fluxes. For the case of deep, dense clouds, the satellite brightness temperature gives guidance as to where the cloud-top height is actually located for comparison with the lidar-measured "effective" cloud top. The reflected solar radiance, when corrected for bidirectional effects, gives a measure of the cloud albedo, from which can be derived, with the use of theoretical relationships, the cloud optical depth. However, in that case, care has to be taken to differentiate between ice cloud and water cloud albedo–optical depth relationships (e.g., Platt et al. 1980). The Platt et al. (1980) paper illustrates, in fact, that the problem can be inverted for semitransparent clouds, so that satellite-derived reflectances can be compared against lidar- or radiometer-derived optical depths. It should be noted that the AVHRR 3.7-μm channel, although it tends to be noisy for some satellites, can give valuable additional information on cloud particle size and phase (e.g., Arking and Childs 1985), which can again be compared with lidar data.

8. All-sky camera and video data

The use of an all-sky camera or even a directional video camera has also been encouraged. Such supporting observations can give a visible image of a cloud, its brokenness, and its texture. The velocity of the clouds can also be calculated, given the movement of the cloud images from one frame to the next plus the cloud-base height measurement from the lidar.

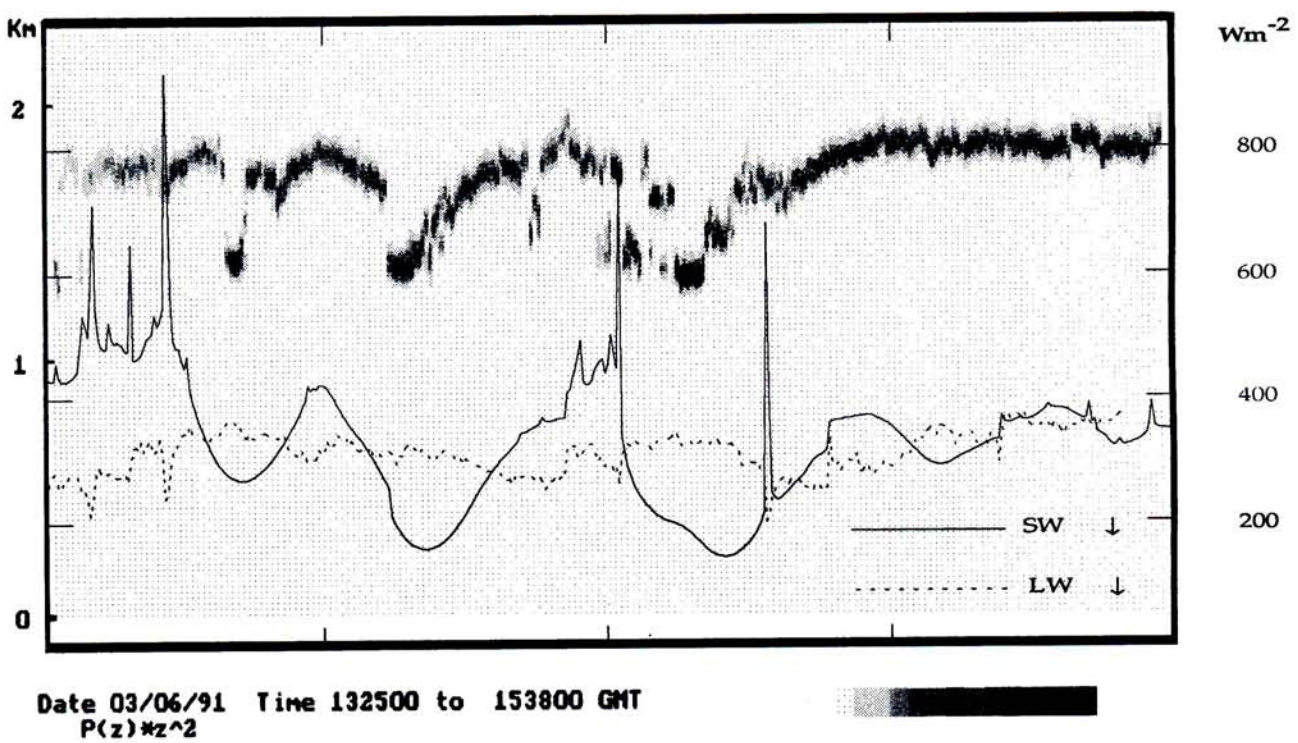

FIG. 11. Downcoming visible and infrared fluxes at the ground below a field of boundary layer clouds, containing occasional gaps and two cloud-base levels. Cloud-base backscatter is illustrated by the grayscale. The considerable variability of ground fluxes under these conditions is evident (Flamant, private communication).

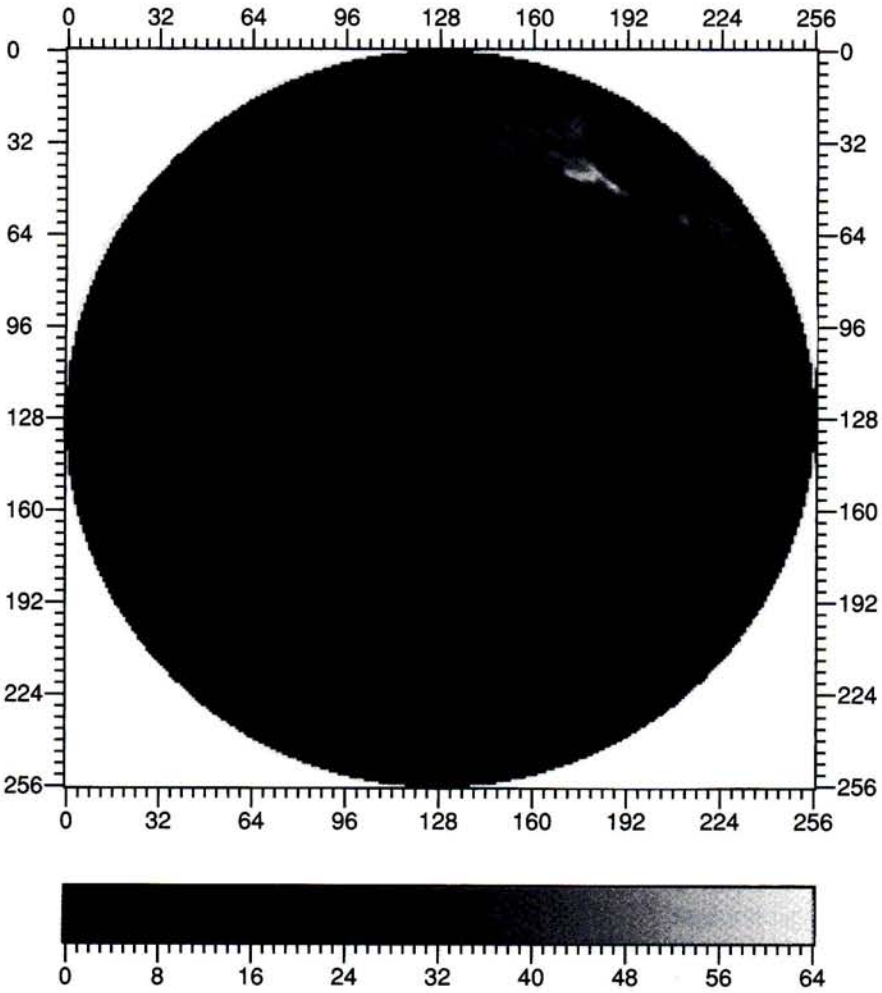

FIG. 12. An all-sky image taken at one time for a day of midlevel to high clouds. The image was taken at 1540:00 Australian eastern standard time (AEST) on 27 June 1991 during ECLIPS II at Aspendale (i.e., C. M. Platt in Table 2). It is a digital image acquired through a 150° field-of-view lens with an equidistant projection. The image has a resolution of 256 x 257 pixels, with 64 gray shades giving pixel values rather than images. The instantaneous lidar profiles gave cloud-base and cloud-top heights at 4.3 km and 6.0 km, respectively (Wooldridge, private communication).

One useful feature of the cloud images is that they provide a measure of both cloud brokenness and amount, and cloud optical depth variations, the latter from the variable cloud brightness. With some assumptions, these features can be integrated to give modeled shortwave and longwave fluxes at the ground for comparison with the observed values and their variation with time (e.g., see section 5).

A typical all-sky camera image of clouds is shown in Fig. 12 together with the cloud heights measured simultaneously. Figure 13 shows the cloud amounts and the longwave and shortwave (solar) fluxes for the entire period of daylight on the same day. These data illustrate their potential usefulness for studying the dependence of surface fluxes on cloud properties, particularly when combined with lidar data.

9. Conclusions

The ECLIPS project has shown, quite successfully, that there is a wealth of material available using a few carefully chosen ground-based instruments. ECLIPS promises to yield useful data on cloud-base altitude statistics and their geographical variation, cloud optical depths and extinction, surface fluxes, and satellite radiances. Such datasets will be valuable for the development of more accurate algorithms to recover global surface fluxes from satellite data, as well as giving valuable data on optical depths and cloud heights for climate model simulations.

As stated by the Working Group on Radiative Fluxes (WMO 1992), the determination of the surface longwave radiation budget is likely to be advanced by the "hybrid approach," which would use model results for a first-guess field, amended by satellite radiance and surface radiation measurements. With the addition of lidar to give accurate cloud-base heights and structures, it is evident that ECLIPS data will be ideal for these approaches.

The correlation of cloud optical properties, such as cloud absorption coefficient, with temperature has already been demonstrated to give useful relationships for ice clouds (Platt and Harshvardhan 1988), which are now being applied empirically to numerical models (e.g., Molnar and Wang 1992). ECLIPS will provide an excellent opportunity to extend the database on such correlations as well as cover a greater range of cloud types and climatic locations.

10. Plans for ECLIPS

Future plans for ECLIPS were discussed at both the fourth ECLIPS meeting in Toronto, May 1992, and the fifth ECLIPS meeting in Salt Lake City, March 1993.

Because of sustained enthusiasm for and interest

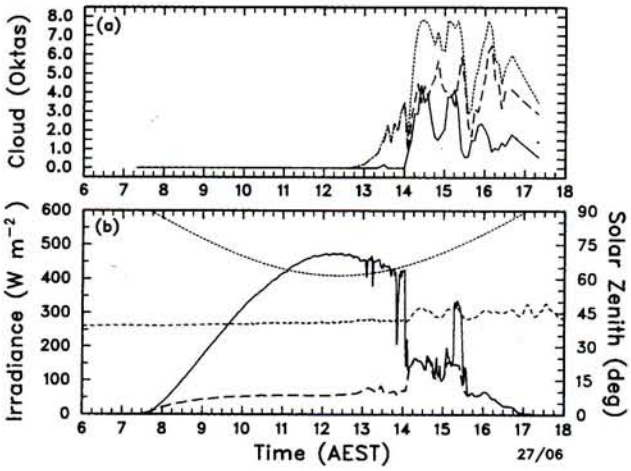

FIG. 13. (a) Cloud amount in oktas for 27 June 1991, deduced from images such as that shown in Fig. 12. Cloud amounts were estimated using a 69-sector equal-area analysis of a color positive whole-sky image using a binary cloud retrieval methodology. Total cloud amount: dotted line; thin cloud: dashed line; opaque cloud: solid line (Wooldridge). (b) Surface fluxes measured on 27 June 1991. Solar zenith angle: dotted line; longwave irradiance: small dashed line; diffuse solar irradiance: large dashed line; global solar irradiance: full line (Wooldridge, private communication).

in ECLIPS, it was generally agreed, at the Toronto meeting, that ECLIPS should continue. This led to an agreement at Salt Lake City that an ECLIPS III observation period should take place. The timing for ECLIPS Phase III was not decided on at the meeting, although there were two suggestions. First, it should be timed to coincide with the NASA LITE (Lidar-in-space Technology Experiment) shuttle project due for launch in September 1994. Second, it should be arranged to cover an intermediate season (autumn/spring) between the previous summer/winter phases. It is possible that if LITE is indeed launched in September 1994, then both the above requirements can be achieved simultaneously. Plans will be firmed up in early 1994. Close association with the BSRN, the ARM program, and Gewex Cloud System Study is seen as essential.

ECLIPS methods also show promise for long-term cloud monitoring to supplement the larger, more comprehensive ARM Cloud and Radiation Testbed (CART) sites. Bearing in mind that ECLIPS has been a low-cost effort, with little money earmarked specifically for the program, further ECLIPS activities in the form of long-term monitoring will require a commitment from respective governments, but the rewards should easily pay for a modest outlay.

Expansion of ECLIPS-type observations can be envisaged with the addition of further instrumentation, such as is planned at the ARM CART sites. Millimeter radars will enhance information at the CART sites considerably as radar pulses generally penetrate to the top of dense water clouds. However, there is also considerable merit in developing monitoring stations with the present ECLIPS arrangement, because monitoring could then be carried out at many more stations than might otherwise be the case.

Acknowledgments. The program acknowledges the assistance given by the International Radiation Commission and the International Committee for Laser Atmospheric Studies in the initial setting up of the program. The part played by Dr. R. Schiffer is recognized with gratitude. Thanks are due to NASA Langley Research Center for agreeing to house the data archive. Participants in the program would like to acknowledge the support of their institutions and to recognize the contributions of many others, too numerous to name, who assisted with the experiments. The assistance given by Dr. G. L. Stephens in the early formulation of the project is also acknowledged.

Appendix A

ECLIPS Landmarks

1984 A request from the International Radiation Commission for expressions of interest in participating in cloud-base monitoring was received and put to the 13th International Laser Radar Conference (ILRC) in August 1984. Some interest was registered and a questionnaire was circulated.

1985 A meeting of experts discussed the concept of lidar networking at a WMO workshop in Geneva, Switzerland, December 1985. The idea of cloud monitoring was approved in principle (WMO 1985).

1988 A workshop on cloud-base measurement was held at Commonwealth Scientific and Industrial Research Organisation, Aspendale, Australia, March 1988, where the plan for a pilot study (ECLIPS) was conceived (WMO 1988).

1989 A second workshop was held in February 1989, at Hampton, Virginia, to plan the experimental phases of ECLIPS. A statement of the plan was circulated to possible participants.

1989 The first intensive field experiment was held in September to December (Phase I).

1990 The third ECLIPS workshop, Porano, Italy, October 1990, planned for the second intensive phase and discussed ECLIPS algorithms, data format, etc.

1991 The second intensive field experiment was held from April to June (Phase II).

1992 The fourth ECLIPS Workshop, Toronto, May

1992, planned for dissemination of results, archiving of data and longer-term observations.

1993 The fifth ECLIPS meeting, Salt Lake City, March 1993, planned for a comparison and consolidation of extinction retrieval methods for publication, and also for a third intensive field experiment (Phase III).

Note: Reports on the first to fourth workshops and the March 1993 meeting are available from C. M. Platt.

Appendix B

ECLIPS Data Archive

A data archive has been established at NASA Langley Research Center. Several editions of a data format report have been produced over the past few years by the ECLIPS science team. The latest edition, together with other information, is available from the following address:

ECLIPS Data Manager
Aerosol Research Branch M/S 475
NASA Langley Research Center
Hampton, VA 23681–0001.

The data that have been archived comprise a very complete list of site information, lidar class, surface infrared and visible instrumentation, surface meteorological information, time of observations, radiosonde data available, satellite type, and spectral channel and associated observational data. These data streams are listed below.

1) Site name
2) Site address
3) Site parameters
4) Transmitter type
5) Transmitter parameters
6) Receiver parameters
7) Pyrgeometer parameters
8) Radiosonde parameters
9) Other radiometer parameters
10) Satellite parameters
110) Channel parameters
90) Microwave water radiometer parameters
11) Surface observations
12) Cloud lidar data
13) Longwave data
113) Shortwave data
14) Radiosonde data
15) Extinction coefficient data
16) Extinction coefficient data—averages
17) Depolarization ratio data
18) Depolarization ratio data—averages
19) Emittance data
20) Calibration constant data
91) Narrow field infrared radiometer data
92) Microwave water radiometer* data

*These data are available from one site (W. Eberhard et al. 1992).

Data observed at individual sites are summarized in Table 3.

Note: (i) Satellite data (see section 7). It was intended that satellite data be provided by individual investigators interested in validating their satellite retrievals. However, satellite data have been archived locally by certain stations. Please contact C. M. Platt for details.

(ii) All-sky camera and video data. These data were recorded by most stations as illustrated under "video" in Table 3. The data have not been archived as yet, but are available from individual investigators.

References

Arking, A., and J. D. Childs, 1985: Retrieval of cloud cover parameters from multispectral satellite images. *J. Appl. Meteor.*, **24,** 322–333.

Ansmann, A., U. Wandinger, M. Riebesell, C. Weitkamp, and W. Michaelis, 1992: Independent measurement of extinction and backscatter profile in cirrus clouds by using a combined Raman elastic-backscatter lidar. *Appl. Opt.*, **31,** 7113–7131.

Barrett, E. W., and O. Ben-Dov, 1967: Application of the lidar to air pollution measurements. *J. Appl. Meteor.*, **6,** 500–515.

Bissonnette, L. R., 1986: Sensitivity analysis of lidar inversion algorithms. *Appl. Opt.*, **25,** 2122–2125.

Brogniez, G., J. Buriez, C. Vanhoutte, and Y. Fouquart, 1986: An improvement of the calibration of the Eppley pyrgeometer for the case of airborne measurements. *Beitr. Phys. Atmos.*, **59,** 538–551.

Carnuth, W., and R. Reiter, 1986: Cloud extinction profile measurements by lidar using Klett's inversion method. *Appl. Opt.*, **25,** 2899–2907.

Cess, R. D., G. L. Potter, J. P. Blanchet, G. J. Boer, S. J. Ghan, J. T. Kiehl, H. Le Treut, Z. X. Li, X. Z. Liang, J. F. B. Mitchell, J.-J. Morcrette, D. A. Randall, M. R. Riches, E. Roeckner, U. Schlese, A. Slingo, K. E. Taylor, W. M. Washington, R. T. Wetherald, and I. Yagai, 1989: Interpretation of cloud climate feedback as produced by 14 atmospheric general circulation models. *Science,* **245,** 513–516.

Davis, P. A., 1969: The analysis of lidar signatures of cirrus clouds. *Appl. Opt.*, **8,** 2099–2102.

Del Guasta, M., M. Morandi, L. Stefanutti, J. Brechet, and J. Piquad, 1993: One year of cloud lidar data from Dumont D'Urville (Antarctica). I. General overview of geometrical and optical properties. *J. Geophys. Res.*, **98,** 18 575–18 587.

Eberhard, W. L., 1993a: Dual-wavelength CO_2 lidar method for distinguishing ice, water, and mixed-phase clouds. *Optical Re-*

mote Sensing of the Atmosphere Technical Digest, Opt. Soc. Amer., 106–109.

——, 1993b: CO_2 lidar techniques for observing characteristic drop size in water clouds. *IEEE Trans. Geosci. Remote Sens.,* **31,** 56–63.

——, T. Uttal, K. A. Clark, R. E. Cupp, E. G. Dutton, L. S. Fedor, J. M. Intrieri, S. Y. Matrosov, J. G. Snider, and R. J. Willis, 1992: Remote sensing data from CLARET: A prototype CART data set. NOAA Tech. Memo., ERL WPL-223, 58 pp.

Fernald, F. G., 1984: Analysis of atmospheric lidar observations: Some comments. *Appl. Opt.,* **23,** 652–654.

——, B. M. Herman, and J. A. Reagon, 1972: Determination of aerosol height distributions by lidar. *J. Appl. Meteor.,* **11,** 482–489.

Gras, J. L., C. M. R. Platt, W. D. Jones, R. M. Huffaker, S. A. Young, S. M. Banks, and D. J. Booth, 1991: Southern Hemisphere tropospheric aerosol backscatter measurements: Implications for a laser wind system. *J. Geophys. Res.,* **96**(D3), 5357–5367.

Intrieri, J. M., G. L. Stephens, W. L. Eberhard, and T. Uttal, 1993: A method for determining cirrus cloud particle sizes using lidar and radar backscatter technique. *J. Appl. Meteor.,* **32,** 1074–1082.

Klett, J. D., 1981: Stable analytical inversion solution for processing lidar returns. *Appl. Opt.,* **20,** 211–220.

Kolev, I., O. Parvanov, B. Kaprielov, and S. Kolev, 1989: Lidar observation of time and spatial variations of backscattering coefficient near the stratiform cloud base. *Atmos. Res.,* **24,** 13–32.

——, ——, ——, and Y. Tomova, 1993: Lidar cloud observation: In part of ECLIPS phase II in the region of Sofia. *Optical Remote Sensing of the Atmosphere Technical Digest,* Series Vol. 5, Opt. Soc. of America, 130–133.

Lindberg, J. D., W. J. Lentz, E. M. Measure, and R. Rubio, 1984: Lidar determinations of extinction in stratus clouds. *Appl. Opt.,* **23,** 2172–2177.

Minnis, P., D. F. Young, K. Sassen, J. M. Alvarez, and C. J. Grund, 1990: The 27–28 October 1986 FIRE IFO cirrus case study: Cirrus parameter relationships derived from satellite and lidar data. *Mon. Wea. Rev.,* **118,** 2402–2425.

Mitchell, J. F. B., C. A. Senior, and W. J. Ingram, 1989: CO_2 and climate: A missing feedback? *Nature,* **341,** 132–134.

Molnar, G., and W.-C. Wang, 1992: Effects of cloud optical property feedbacks on greenhouse warming. *J. Climate,* **5,** 814–820.

Pal, S. R., W. Steinbrecht, and A. I. Carswell, 1992: Automated method for lidar determination of cloud base height and vertical extent. *Appl. Opt.,* **31,** 1488–1494.

Platt, C. M. R., 1973: Lidar and radiometric observations of cirrus clouds. *J. Atmos. Sci.,* **30,** 1191–1204.

——, 1979: Remote sounding of high clouds. I: Of visible and infrared optical properties from lidar and radiometer measurements. *J. Appl. Meteor.,* **18,** 1130–1143.

——, 1981: Remote sounding of high clouds. III: Monte Carlo calculations of multiple scattered lidar returns. *J. Atmos. Sci.,* **38,** 156–167.

——, and K. Bartusek, 1974: Structure and optical properties of some midlevel clouds. *J. Atmos. Sci.,* **31,** 1079–1088.

——, and G. L. Stephens, 1980: The interpretation of remotely sensed high cloud emittances. *J. Atmos. Sci.,* **37,** 2314–2322.

——, and Harshvardhan, 1988: Temperature dependence of cirrus extinction: Implications for climate feedback. *J. Geophys. Res.,* **93,** 11 051–11 058.

——, D. W. Reynolds, and N. L. Abshire, 1980: Satellite and lidar observations of the albedo emittance and optical depth of cirrus compared to model calculations. *Mon. Wea. Rev.,* 195–204.

——, J. C. Scott, and A. C. Dilley, 1987: Remote sounding of high clouds. VI: Optical properties of midlatitude and tropical cirrus. *J. Atmos. Sci.,* **44,** 729–747.

——, S. A. Young, G. R. Patterson, and P. J. Manson, 1993: Lidar and radiometer observations of midlevel clouds. *Optical Remote Sensing of the Atmosphere Technical Digest,* Series Vol. 5. Opt. Soc. America, 114–117.

Qiu, 1988: Sensitivity of lidar equation solution to boundary values and determination of the values. *Adv. Atmos. Sci.,* **5,** 229–241.

Roeckner, E., U. Schlese, J. Biercamp, and P. Loewe, 1987: Cloud optical depth feedbacks and climate modeling. *Nature,* **329,** 138–140.

Sassen, K., and B. S. Cho, 1992: Subvisual-thin cirrus lidar dataset for satellite verification and climatological Research. *J. Appl. Meteor.,* **31,** 1275–1285.

——, and H. Zhao, 1993: Supercooled liquid water clouds in Utah winter mountain storms: Cloud seeding implications of a remote sensing dataset. *J. Appl. Meteor.,* **32,** 1548–1558.

——, ——, and G. C. Dodd, 1992: Simulated polarization diversity lidar returns from water and precipitating mixed phase clouds. *Appl. Opt.,* **31,** 2914–2923.

Stone, R. S., G. L. Stephens, C. M. R. Platt, and S. Banks, 1990: The remote sensing of thin cirrus cloud using satellites, lidar and radiative transfer theory. *J. Appl. Meteor,* **29,** 353–366.

Viezee, W., E. E. Uthe, and R. T. H. Collis, 1969: Lidar observations of airfield approach conditions. *J. Appl. Meteor.,* **8,** 274–283.

WMO, 1985: Aerosols, clouds and other climatically important parameters: Lidar applications and networks. Rep. WMO/TD-No. 233.

——, 1988: An experimental cloud lidar pilot study (ECLIPS). Report of the WCRP/CSIRO Workshop on Cloud Base Measurement, 1988, WMO/TD-No. 251.

——, 1992: Radiation and climate. Report of the Fourth Session of the WCRP Working Group on Radiative Fluxes, WMO/TD-No. 471, 47 pp.